

Influence Maximization based on Threshold Models in Hypergraphs

Renquan Zhang,¹ Xilong Qu,¹ Qiang Zhang,² Xirong Xu,² and Sen Pei^{*3}

¹*School of Mathematical Sciences, Dalian University of Technology*

²*School of Computer Science and Technology, Dalian University of Technology*

³*Department of Environmental Health Sciences, Mailman School of Public Health, Columbia University*

(*Electronic mail: sp3449@cumc.columbia.edu.)

(Dated: 23 November 2023)

Influence Maximization problem has received significant attention in recent years due to its application in various domains such as product recommendation, public opinion dissemination, and disease propagation. This paper proposes a theoretical analysis framework for collective influence in hypergraphs, focusing on identifying a set of seeds that maximize influence in threshold models. Firstly, we extend the Message Passing method from pairwise networks to hypergraphs to accurately describe the activation process in threshold models. Then we introduce the concept of hypergraph collective influence (HCI) to measure the influence of nodes. Subsequently, we design an algorithm, HCI-TM, to select the Influence Maximization Set, taking into account both node and hyperedge activation. Numerical simulations demonstrate that HCI-TM outperforms several competing algorithms in synthetic and real-world hypergraphs. Furthermore, we find that HCI can be used as a tool to predict the occurrence of cascading phenomena. Notably, we find that HCI-TM algorithm works better for larger average hyperdegrees in Erdős-Rényi (ER) hypergraphs and smaller power-law exponents in scale-free (SF) hypergraphs.

The innovation of this study lies in several key aspects. Firstly, we extend the Message Passing equation to threshold models in hypergraphs, providing a more comprehensive and accurate understanding of the activation process. Secondly, we introduce the concept of Hypergraph Collective Influence (HCI), which quantifies the collective influence of nodes in hypergraphs. HCI offers a novel approach to measuring the influence potential of individual nodes in hypergraphs. Thirdly, we propose the HCI-TM algorithm, designed to select the Influence Maximization Set in hypergraphs based on threshold models. Notably, the HCI-TM algorithm considers both individual node influence and the collective impact of hyperedges, resulting in more effective Influence Maximization strategies in hypergraphs. Through extensive simulations on synthetic and real-world hypergraphs, we demonstrate that the HCI-TM algorithm outperforms other classical algorithms. Additionally, HCI proves useful in predicting cascading phenomena. Furthermore, our simulations reveal interesting observations, indicating that the HCI-TM algorithm performs better with larger average hyperdegrees in ER hypergraphs and smaller power-law exponents in SF hypergraphs. These findings provide valuable insights into the influence of hypergraph characteristics on HCI-TM algorithm performance.

shape public opinion, thereby facilitating the transmission of ideas. Similarly, identifying and immunizing super spreaders in disease transmission networks is crucial for effectively containing outbreaks. Due to its broad applications in disease control^{5,6}, marketing strategy⁷, and other fields⁸, this problem has emerged as a prominent topic in recent academic research.

In pairwise networks, the topic of Influence Maximization has been extensively researched^{9,10}, and a large number of heuristic algorithms, such as Betweenness¹¹, High Degree (HD)¹², PageRank¹³, K-core¹⁴, and CI¹⁵⁻¹⁷, have been presented. However, with the continuous development of complex system modeling¹⁸, researchers are increasingly realizing that many real-world interactions involve multiple individuals. Pairwise networks are difficult to distinguish and describe high-order interactions. For example, a research group can consist of multiple members, a WeChat group can have multiple participants, and a tweet can receive multiple comments. Hypergraphs provide a modeling framework that can distinguish and represent such high-order interactions^{19,20}. In recent years, with the growing development of hypergraph theory and its wide-ranging applications, there has been a greater interest in Influence Maximization problem in hypergraphs. Xie et al.²¹ proposed an effective adaptive heuristic algorithm to find the optimal set of influence seeds in hypergraphs. Zhu et al.²² investigated how to maximize social influence in social hypergraphs. Austin R. et al.²³ extended the feature vector center from graphs to hypergraphs. These²¹⁻²⁵ are important progress on Influence Maximization problem in hypergraphs. However, it remains a challenging problem, as many existing heuristic algorithms lack sufficient mathematical analysis and overlook the dependence of nodes' neighbors. It is widely recognized that the Message Passing equation²⁶ has proven effective in reducing loops in pairwise networks by removing nodes, enhancing node independence, and providing a more precise definition of the information transmission process. In this study, we aim to extend the existing theory to hypergraphs in order to investigate the Influence Maximization problem.

I. INTRODUCTION:

The Influence Maximization problem in complex networks, which aims to select a fixed number of seed nodes to maximize the scope of spreading, is widely recognized as an NP-hard problem^{1,2}. The critical role played by a small subset of nodes in the spreading process has been widely acknowledged in various applications^{3,4}. For instance, a limited number of individuals possess significant influence and can

Our main contribution lies in the proposal of a novel Message Passing equation tailored specifically for threshold models in hypergraphs, thereby providing a more effective framework for analyzing and optimizing influence propagation in hypergraphs.

Linear Threshold Models (LTM) can describe a large variety of real-world phenomena, such as disease spread²⁷, public opinion diffusion²⁸, information dissemination²⁹, and behavior adoption^{1,30,31}. However, there haven't been many studies³² on threshold models in hypergraphs up to now. Therefore, we aim to investigate the optimal influence of nodes based on the threshold models in hypergraphs. The main contributions of this paper are as follows:

- In this paper, we extend the Message Passing Method from pairwise networks to hypergraphs in order to reduce the dependence of nodes' neighbors. Then we analyze the self-satisfying equation to obtain the Hypergraph Collective Influence (HCI), which serves as a metric for quantifying the collective influence of nodes in hypergraphs.
- To select the optimal influence node in hypergraphs, we propose the HCI-TM algorithm. Compared to other methods, our algorithm not only maximizes node activation scale but also hyperedge activation scale.
- Through numerical simulations, we demonstrate that the HCI-TM algorithm outperforms other classical algorithms in both synthetic hypergraphs and real-world hypergraphs. Additionally, we find that HCI can be used as a basis for assessing the occurrence of cascade phenomena.
- Our numerical simulations further reveal that larger average hyperdegrees in ER hypergraphs and smaller power-law exponents in SF hypergraphs could enhance the performance of HCI-TM algorithm.

The article structure is as follows: Section 1 provides the background, research motivation, and innovative aspects of our study. In Section 2, we introduce the threshold models in hypergraphs. Section 3 focuses on extending the Message Passing Method from pairwise networks to hypergraphs. We propose the concept of HCI and design the HCI-TM algorithm to select the Influence Maximization Set based on threshold models in hypergraphs. Section 4 presents the validation of the HCI-TM algorithm through numerical simulations conducted on both synthetic and real-world hypergraphs. The results demonstrate the superiority and robustness of HCI-TM in diverse hypergraph structures. And we also find that HCI can be used as a tool to predict the occurrence of cascading phenomenon. Finally, in Section 5, we summarize our findings and provide insightful suggestions for future research directions.

II. THRESHOLD MODELS IN HYPERGRAPHS:

A hypergraph is a generalization of a graph where a hyperedge can connect any number of nodes, unlike regular graphs

which only allow connections between two nodes. Hypergraph $\mathbb{H} = (V, E)$ is a subset system of finite sets, where V is the set of nodes in the hypergraph, and E is the set of hyperedges in the hypergraph. In a hypergraph with N nodes and M hyperedges, the topology structure can be represented by the correlation matrix $\{H_{ie_\gamma}\}_{N \times M}$. Here, H_{ie_γ} is equal to 1 if node i is associated with hyperedge e_γ , and 0 otherwise. We use vector $\mathbf{n} = (n_1, n_2, \dots, n_N)^T$ to indicate whether node i is a seed node. If node i is a seed node, the i th component $n_i = 1$, otherwise, $n_i = 0$. So the fraction of seed nodes $q = \sum_{i=1}^N \frac{n_i}{N}$. During the activating process, the states of each node and hyperedge can be either active or inactive, depending on the rule of threshold models in hypergraphs. Assuming that hyperedge e_γ consists of N_γ nodes and m_γ nodes of them are in the state of active. The hyperedge e_γ becomes activated if the fraction of activated nodes $\frac{m_\gamma}{N_\gamma}$ reached or exceeded the threshold value $t_\gamma \in (0, 1)$. Once a hyperedge becomes activated, all the nodes within that hyperedge will also become active in the next step of the propagation process. This process continues until there are no more newly activated nodes or hyperedges. To illustrate this concept, we can refer to Fig.(1), which shows an example of the activation process in a hypergraph. In this example, all the threshold values of the hyperedges are set to $t_\gamma = 0.5$, meaning that a hyperedge becomes activated when at least half of its nodes are already active. At the initial time $t = 0$, node 3 is chosen as the initial seed, so $U(0) = \{3\}$. Depending on the threshold rule, the hyperedges e_{γ_2} and e_{γ_3} get activated at time $t = 1$ because their fractions of activated nodes reached threshold 0.5, so $U(1) = \{3, e_{\gamma_2}, e_{\gamma_3}\}$. At time $t = 2$, nodes 2 and 6 are made to activated subsequently and $U(2) = \{3, e_{\gamma_2}, e_{\gamma_3}, 2, 6\}$. At next step, the hyperedges e_{γ_1} and e_{γ_5} are both activated, making nodes 1 and 7 activated respectively, so $U(3) = \{3, e_{\gamma_2}, e_{\gamma_3}, 2, 6, e_{\gamma_1}, e_{\gamma_5}\}$ and $U(4) = \{3, e_{\gamma_2}, e_{\gamma_3}, 2, 6, e_{\gamma_1}, e_{\gamma_5}, 1, 7\}$. Since no more nodes or hyperedges will be activated, this propagation process ends at time $t = 4$.

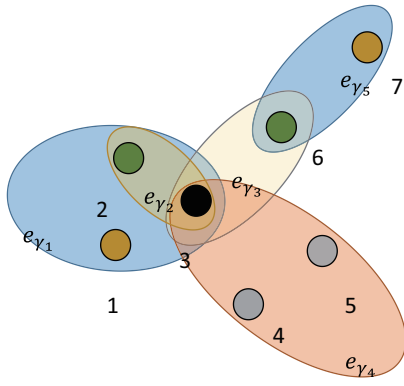
In this paper, all thresholds of the hyperedges are set to the same value, which range from 0.5 to 0.8.

III. THEORETICAL ANALYSIS AND HCI-TM ALGORITHM

In this Section, we propose a collective influence theoretical analysis framework based on threshold models in hypergraphs.

A. Message Passing Equation

In the spread process, v_i represents the probability of node i being activated, and v_{e_γ} the probability of hyperedge e_γ being activated. At the final stage of propagation, v_i and v_{e_γ} can only show two states, that is, $v_i = 0$ ($v_{e_\gamma} = 0$), indicating that node i (hyperedge e_γ) has not been activated, and $v_i = 1$ ($v_{e_\gamma} = 1$), indicating that node i (hyperedge e_γ) has been activated.



- Step 0: $U(0) = \{3\}$
 Step 1: $U(1) = \{3, e_{\gamma_2}, e_{\gamma_3}\}$
 Step 2: $U(2) = \{3, e_{\gamma_2}, e_{\gamma_3}, 2, 6\}$
 Step 3: $U(3) = \{3, e_{\gamma_2}, e_{\gamma_3}, 2, 6, e_{\gamma_1}, e_{\gamma_5}\}$
 Step 4: $U(4) = \{3, e_{\gamma_2}, e_{\gamma_3}, 2, 6, e_{\gamma_1}, e_{\gamma_5}, 1, 7\}$

FIG. 1. The diagram of the hypergraph spread process depicts nodes as circles and hyperedges as ovals. Each hyperedge comprises multiple nodes, and each node is associated with multiple hyperedges. The colors assigned to the hyperedges and nodes represent the order of activation.

Therefore, we denote $Q(q) = \frac{\sum_{i=1}^N v_i}{N}$ as the final proportion of the active nodes with size q of the initial seed nodes.

In hypergraph, the Cavity Method can be extended to the "link" between node and hyperedge. Actually, the hypergraph can be described as a Bipartite Graph, which consist of two kinds of node: the nodes and hyperedges in hypergraph are both taken as the node in Bipartite Graph, the links in Bipartite Graph only exist between node and hyperedge when they are associated in hypergraph. So we can consider to remove two kinds of node in Bipartite Graph by Cavity Method. For a directed link from node i to hyperedge e_γ , suppose e_γ is "virtually" removed from the Bipartite Graph and reconsider if node i is activated or not. The variable $v_{i \rightarrow e_\gamma}^t$ represents the probability of node i being activated in the absence of hyperedge e_γ at time t . Similarly, $v_{e_\gamma \rightarrow i}^t$ represents the probability of hyperedge e_γ being activated in the absence of node i at time t . Notice that although the direct impact between node i and hyperedge e_γ did not occur, they can still affect each other by a longer path $i \leftrightarrow e_\beta \leftrightarrow \dots \leftrightarrow j \leftrightarrow e_\gamma$. For sparse hypergraphs, the updating process can be obtained:

$$\begin{cases} v_{i \rightarrow e_\gamma}^{t+1} = n_i + (1 - n_i) \left[1 - \prod_{e_\beta \in \partial i / e_\gamma} (1 - v_{e_\beta \rightarrow i}^t) \right] \\ v_{e_\gamma \rightarrow i}^{t+1} = 1 - \prod_{P_h \in P_{e_\gamma/i}^{m_\gamma}} \left(1 - \prod_{p \in P_h} v_{p \rightarrow e_\gamma}^t \right) \end{cases} \quad (1)$$

Here, $\partial i / e_\gamma$ represents the set of hyperedges related to node i except e_γ . $P_{e_\gamma/i}^{m_\gamma} = \{P_1, P_2, \dots, P_\tau\}$ is defined as the set of all combinations of m_γ nodes in hyperedge e_γ excluding node i , where $\tau = C_{N_\gamma-1}^{m_\gamma}$. Each element P_h in $P_{e_\gamma/i}^{m_\gamma}$ has

the form $P_h = \{p_{h_1}, p_{h_2}, \dots, p_{h_{m_\gamma}}\}$, representing the h th combination composed of m_γ nodes. Notice that in Eq.(1), the states of $v_{i \rightarrow e_\gamma}^t$ and $v_{e_\gamma \rightarrow i}^t$ will update every two time steps (i.e. $v_{i \rightarrow e_\gamma}^{2t+1} = v_{i \rightarrow e_\gamma}^{2t}$ and $v_{e_\gamma \rightarrow i}^{2t+2} = v_{e_\gamma \rightarrow i}^{2t+1}$ for all $t = 0, 1, \dots$). Denote $\lim_{t \rightarrow \infty} v_{i \rightarrow e_\gamma}^t = v_{i \rightarrow e_\gamma}$ and $\lim_{t \rightarrow \infty} v_{e_\gamma \rightarrow i}^t = v_{e_\gamma \rightarrow i}$. The message passing equations can be described as:

$$\begin{cases} v_{i \rightarrow e_\gamma} = n_i + (1 - n_i) \left[1 - \prod_{e_\beta \in \partial i / e_\gamma} (1 - v_{e_\beta \rightarrow i}) \right] \\ v_{e_\gamma \rightarrow i} = 1 - \prod_{P_h \in P_{e_\gamma/i}^{m_\gamma}} \left(1 - \prod_{p \in P_h} v_{p \rightarrow e_\gamma} \right) \end{cases} \quad (2)$$

Moreover, the final state of node i and hyperedge e_γ is given as follows:

$$\begin{cases} v_i = n_i + (1 - n_i) \left[1 - \prod_{e_\beta \in \partial i} (1 - v_{e_\beta \rightarrow i}) \right] \\ v_{e_\gamma} = 1 - \prod_{P_h \in P_{e_\gamma}^{m_\gamma}} \left(1 - \prod_{p \in P_h} v_{p \rightarrow e_\gamma} \right) \end{cases} \quad (3)$$

B. High-order Collective Influence

To simplify the Eq.(2), let's denote $\mathbf{V}_\rightarrow = \{\mathbf{v}_1, \mathbf{v}_2\}^T$, where $\mathbf{v}_1 = \{v_{i \rightarrow e_\gamma}\}_{S \times 1}$, $\mathbf{v}_2 = \{v_{e_\gamma \rightarrow i}\}_{S \times 1}$. Here $S = \sum_{i=1}^N k_i$ and k_i represents the hyperdegree of node i . Correspondingly, we extend \mathbf{n} to \mathbf{n}_\rightarrow with larger dimension $2S$:

$$\mathbf{n}_\rightarrow = (\mathbf{n}_1, \mathbf{0})^T = (\underbrace{\dots, n_i, \dots, n_i, \dots}_S, \underbrace{0, \dots, 0}_S)^T \quad (4)$$

So the Eq.(2) can be described as a nonlinear function:

$$\mathbf{V}_\rightarrow = \mathbf{n}_\rightarrow + \mathcal{G}(\mathbf{V}_\rightarrow) \Leftrightarrow \begin{cases} \mathbf{v}_1 = \mathbf{n}_1 + \mathbf{g}_1(\mathbf{v}_2) \\ \mathbf{v}_2 = \mathbf{0} + \mathbf{g}_2(\mathbf{v}_1) \end{cases} \quad (5)$$

The final state of \mathbf{V}_\rightarrow is completely determined by giving the initial seeds set \mathbf{n}_\rightarrow , i.e. the solution of the self-consistent Eq.(5) is unique under given initial seeds. Unfortunately, it is hard to solved directly due to the complexity of functions \mathbf{g}_1 and \mathbf{g}_2 ¹⁶, Therefore, we calculate it approximately by iteration and linearization:

$$\mathbf{V}_\rightarrow^{t+1} = \mathbf{n}_\rightarrow + J\mathcal{G}|_{\mathbf{V}_\rightarrow^t} \times \mathbf{V}_\rightarrow^t \quad (6)$$

Here the $J\mathcal{G}|_{\mathbf{V}_\rightarrow^t}$ is the jacobian matrix of Eq.(5) at point \mathbf{V}_\rightarrow^t . For a given hypergraph, we take the partial derivatives of Eq.(5):

$$J\mathcal{G} = \begin{pmatrix} \frac{\partial \mathbf{g}_1}{\partial \mathbf{v}_1} & \frac{\partial \mathbf{g}_1}{\partial \mathbf{v}_2} \\ \frac{\partial \mathbf{g}_2}{\partial \mathbf{v}_1} & \frac{\partial \mathbf{g}_2}{\partial \mathbf{v}_2} \end{pmatrix}_{2S \times 2S} \quad (7)$$

For the partial derivative of \mathbf{g}_1 , We have:

$$\frac{\partial v_{i \rightarrow e_\gamma}}{\partial v_{j \rightarrow e_\beta}} = 0 \quad (8)$$

$$\frac{\partial v_{i \rightarrow e_\gamma}}{\partial v_{e_\beta \rightarrow j}} = \begin{cases} (1 - n_i) \prod_{e_\mu \in \partial i / e_\gamma, e_\beta} (1 - v_{e_\mu \rightarrow i}) & i = j, e_\beta \neq e_\gamma \\ 0 & \text{otherwise} \end{cases} \quad (9)$$

For the first row of jacobian matrix at time t , we have $\frac{\partial \mathbf{g}_1}{\partial \mathbf{v}_1} |_{\mathbf{v}^t} = \mathbf{0}$ and $\frac{\partial \mathbf{g}_1}{\partial \mathbf{v}_2} |_{\mathbf{v}^t} = \left\{ \frac{\partial v_{i \rightarrow e_\gamma}}{\partial v_{e_\beta \rightarrow j}} \right\} |_{\mathbf{v}^t}$ is a generalization of the non-backtracking (NB) matrix, which is only determined by the number of active hyperedges associating to node i except e_γ and e_β at time t , denoted by $a_{e_\beta \rightarrow i, i \rightarrow e_\gamma}^t =$

$\sum_{e_\mu \in \partial i / (e_\gamma, e_\beta)} v_{e_\mu \rightarrow i}^t$. So the $\frac{\partial \mathbf{g}_1}{\partial \mathbf{v}_2}$ can be described as:

$$\frac{\partial v_{i \rightarrow e_\gamma}}{\partial v_{e_\beta \rightarrow j}} |_{\mathbf{v}^t} = \begin{cases} 1 - n_i & i = j, e_\beta \neq e_\gamma, a_{e_\beta \rightarrow i, i \rightarrow e_\gamma}^t = 0 \\ 0 & \text{otherwise} \end{cases} \quad (10)$$

The same analysis on the partial derivative of \mathbf{g}_2 yields that $\frac{\partial v_{e_\gamma \rightarrow i}}{\partial v_{e_\beta \rightarrow j}}$ is always zero and $\frac{\partial v_{e_\gamma \rightarrow i}}{\partial v_{j \rightarrow e_\beta}}$ is almost zero except for $e_\beta = e_\gamma, j \neq i$:

$$\begin{aligned} \frac{\partial v_{e_\gamma \rightarrow i}}{\partial v_{j \rightarrow e_\gamma}} &= \prod_{\substack{P_h \in \mathcal{P}^{m_\gamma} \\ j \notin P_h}} (1 - \prod_{p \in P_h} v_{p \rightarrow e_\gamma}) \\ &\times \sum_{\substack{P_h \in \mathcal{P}^{m_\gamma} \\ j \in P_h}} \left[\prod_{p \in P_h / j} v_{p \rightarrow e_\gamma} \prod_{\substack{\tilde{P}_h \in \mathcal{P}^{m_\gamma} \\ \tilde{P}_h \neq P_h \\ j \in \tilde{P}_h}} (1 - \prod_{p \in \tilde{P}_h} v_{p \rightarrow e_\gamma}) \right] \end{aligned} \quad (11)$$

Although the $\frac{\partial v_{e_\gamma \rightarrow i}}{\partial v_{j \rightarrow e_\gamma}} |_{\mathbf{v}^t}$ seems much complicated, it still can be simplified by the $b_{j \rightarrow e_\gamma, e_\gamma \rightarrow i}^t = \sum_{p \in \partial e_\gamma / (i, j)} v_{p \rightarrow e_\gamma}^t$, which is the number of active nodes associating to e_γ at time t , excluding i and j . Firstly, if $b_{j \rightarrow e_\gamma, e_\gamma \rightarrow i}^t \geq m_\gamma$ at time t , there is at least one combination of P_h that makes for $\prod_{p \in P_h} v_{p \rightarrow e_\gamma}^t = 1$, which leads to that the first part on the right side of Eq.(11) equals zero, so $\frac{\partial v_{e_\gamma \rightarrow i}}{\partial v_{j \rightarrow e_\gamma}} |_{\mathbf{v}^t} = 0$ under this condition. Secondly, if $b_{j \rightarrow e_\gamma, e_\gamma \rightarrow i}^t \leq m_\gamma - 2$ at time t , we have $\prod_{p \in P_h / j} v_{p \rightarrow e_\gamma}^t = 0$ for any combination because at least one zero element will be selected when you choose $m_\gamma - 1$ elements from a set containing at most $m_\gamma - 2$ nonzero elements, so $\frac{\partial v_{e_\gamma \rightarrow i}}{\partial v_{j \rightarrow e_\gamma}} |_{\mathbf{v}^t} = 0$ under this condition. Lastly, only when $b_{j \rightarrow e_\gamma, e_\gamma \rightarrow i}^t = m_\gamma - 1$, there is exactly one combination such that $\prod_{p \in P_h / j} v_{p \rightarrow e_\gamma}^t = 1$. Meanwhile,

all the forms $\prod_{p \in \tilde{P}_h} v_{p \rightarrow e_\gamma}^t$ and $\prod_{p \in P_h} v_{p \rightarrow e_\gamma}^t$ are zeros, which finally leads to $\frac{\partial v_{e_\gamma \rightarrow i}}{\partial v_{j \rightarrow e_\gamma}} |_{\mathbf{v}^t} = 1$. Therefore, for the second row of jacobian matrix at time t , we have $\frac{\partial \mathbf{g}_2}{\partial \mathbf{v}_2} |_{\mathbf{v}^t} = \mathbf{0}$ and another generalized Non-Backtracking matrix $\frac{\partial \mathbf{g}_2}{\partial \mathbf{v}_1} |_{\mathbf{v}^t} = \left\{ \frac{\partial v_{e_\gamma \rightarrow i}}{\partial v_{j \rightarrow e_\beta}} \right\} |_{\mathbf{v}^t}$ described as:

$$\frac{\partial v_{e_\gamma \rightarrow i}}{\partial v_{j \rightarrow e_\beta}} |_{\mathbf{v}^t} = \begin{cases} 1 & e_\beta = e_\gamma, j \neq i, b_{j \rightarrow e_\gamma, e_\gamma \rightarrow i}^t = m_\gamma - 1 \\ 0 & \text{otherwise} \end{cases} \quad (12)$$

For the convenience and simplicity of the following derivation, the jacobian matrix $J^{\mathcal{G}} |_{\mathbf{v}^t}$ is denoted as follows:

$$J^{\mathcal{G}} |_{\mathbf{v}^t} = \begin{pmatrix} \mathbf{0} & \mathcal{M}^t \\ \mathcal{I}^t & \mathbf{0} \end{pmatrix} \quad (13)$$

Here $\mathcal{M}^t = \{ \mathcal{M}_{e_\beta \rightarrow j, i \rightarrow e_\gamma}^t \} = \left\{ \frac{\partial v_{i \rightarrow e_\gamma}}{\partial v_{e_\beta \rightarrow j}} \right\} |_{\mathbf{v}^t}$, $\mathcal{I}^t = \{ \mathcal{I}_{j \rightarrow e_\beta, e_\gamma \rightarrow i} \} |_{\mathbf{v}^t} = \left\{ \frac{\partial v_{e_\gamma \rightarrow i}}{\partial v_{j \rightarrow e_\beta}} \right\} |_{\mathbf{v}^t}$ are the matrix with dimension $S \times S$. We extend the matrices \mathcal{M}^t and \mathcal{I}^t to the higher dimensional space $M \times N \times N \times M$ and $N \times M \times M \times N$. Although they should not be combined to form a matrix because of their different dimensions, it does not affect the subsequent calculation as long as we just do it respectively. Bringing in new symbols:

$$\begin{cases} \mathcal{M}_{e_\beta j i e_\gamma}^t = (1 - n_i) H_{i e_\gamma} H_{j e_\beta} \delta_{ij} (1 - \delta_{e_\beta e_\gamma}) M_{e_\beta i e_\gamma}^t \\ \mathcal{I}_{j e_\beta e_\gamma i}^t = H_{i e_\gamma} H_{j e_\beta} \delta_{e_\beta e_\gamma} (1 - \delta_{ij}) I_{j e_\gamma e_\gamma i}^t \end{cases} \quad (14)$$

Here $M_{e_\beta i e_\gamma}^t$ and $I_{j e_\gamma e_\gamma i}^t$ are the binary matrices. $M_{e_\beta i e_\gamma}^t = 1$ if $a_{e_\beta \rightarrow i, i \rightarrow e_\gamma}^t = 0$ and $M_{e_\beta i e_\gamma}^t = 0$ otherwise. Similarly, $I_{j e_\gamma e_\gamma i}^t = 1$ if $b_{j \rightarrow e_\gamma, e_\gamma \rightarrow i}^t = m_\gamma - 1$ and $I_{j e_\gamma e_\gamma i}^t = 0$ otherwise. The $M_{e_\beta i e_\gamma}^t$ and $I_{j e_\gamma e_\gamma i}^t$ are related to the concept of "subcritical" node and hyperedge respectively. By definition of Ref¹⁶, a node (hyperedge) is subcritical if that one more activation of associated hyperedge (node) will cause it activated. Additionally, $M_{e_\beta i e_\gamma}^t$ and $I_{j e_\gamma e_\gamma i}^t$ are fully determined by $v_{i \rightarrow e_\gamma}^t$ and $v_{e_\gamma \rightarrow i}^t$, implying that both of them are also periodic ($M_{e_\beta i e_\gamma}^{2t+2} = M_{e_\beta i e_\gamma}^{2t+1}$ and $I_{j e_\gamma e_\gamma i}^{2t+1} = I_{j e_\gamma e_\gamma i}^{2t}$ for all $t = 0, 1, \dots$).

For $t = 1$, we set $\mathbf{V}^0 = \mathbf{n}_\rightarrow$, so $\mathbf{V}^1 = \mathbf{n}_\rightarrow + J^{\mathcal{G}^0} \times \mathbf{n}_\rightarrow$:

$$\begin{bmatrix} \mathbf{v}_1 \\ \mathbf{v}_2 \end{bmatrix}^1 = \begin{bmatrix} \mathbf{n}_1 \\ \mathbf{0} \end{bmatrix} + \begin{bmatrix} 0 & \mathcal{M}^0 \\ \mathcal{I}^0 & 0 \end{bmatrix} \begin{bmatrix} \mathbf{n}_1 \\ \mathbf{0} \end{bmatrix} = \begin{bmatrix} \mathbf{n}_1 \\ \mathcal{I}^0 \mathbf{n}_1 \end{bmatrix} \quad (15)$$

Notice that \mathbf{n}_1 should also be extended to the higher dimensional space $N \times M$, based on the Eq.(15), we have:

$$\begin{cases} v_{i \rightarrow e_\gamma}^1 = n_i H_{i e_\gamma} \\ v_{e_\gamma \rightarrow i}^1 = H_{i e_\gamma} \sum_j n_j H_{j e_\gamma} (1 - \delta_{ij}) I_{j e_\gamma e_\gamma i}^0 \end{cases} \quad (16)$$

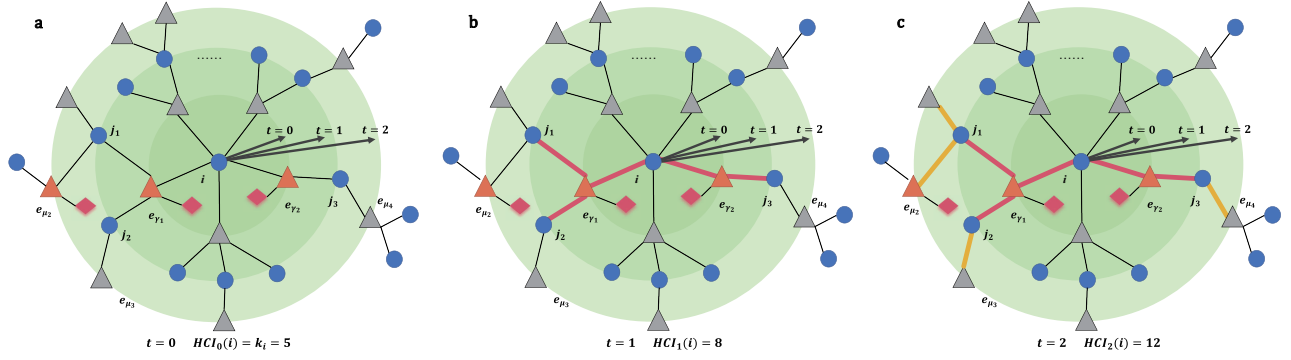


FIG. 2. The illustrates of subcritical path in hypergraphs. The blue circles represent nodes, the triangles represent hyperedges. (a) At $t=0$, $HCI_0(i)$ is equal to the hyperdegree of node i . (b) At $t=1$, the additional 2-length subcritical paths also contribute to $HCI_1(i)$, which represented by thick crimson links. And the orange triangles represent hyperedges in subcritical state, so the $HCI_1(i)=HCI_0(i)+3=8$. (c) At $t=2$, the additional 3-length subcritical paths are represented by thick yellow line, so $HCI_2(i)=HCI_1(i)+4=5+3+4=12$.

Defining $\|v_{\rightarrow}\| = \sum_{ie_{\gamma}}(v_{i \rightarrow e_{\gamma}} + v_{e_{\gamma} \rightarrow i})$ to quantify the activation scale of Threshold Models in hypergraphs, our goal is to optimize the collective influence of a given number of seeds by maximizing $\|v_{\rightarrow}\|$. Based on the Eq.(16), the form of $\|v_{\rightarrow}\|$ for $t=1$ is:

$$\begin{aligned}
 \|v_{\rightarrow}\| &= \sum_{ie_{\gamma}} v_{i \rightarrow e_{\gamma}} + \sum_{ie_{\gamma}} v_{e_{\gamma} \rightarrow i} \\
 &= \sum_{ie_{\gamma}} n_i H_{ie_{\gamma}} + \sum_{ie_{\gamma}} H_{ie_{\gamma}} \sum_j n_j H_{je_{\gamma}} (1 - \delta_{ij}) I_{je_{\gamma}e_{\gamma}i}^0 \\
 &= \sum_i n_i k_i + \sum_i n_i \sum_{e_{\gamma} \in \partial i} \sum_{j \in \partial e_{\gamma}/i} I_{ie_{\gamma}e_{\gamma}j}^0 \\
 &= \sum_i n_i \left(k_i + \sum_{e_{\gamma} \in \partial i} \sum_{j \in \partial e_{\gamma}/i} I_{ie_{\gamma}e_{\gamma}j}^0 \right) \quad (17)
 \end{aligned}$$

Supposing that the final state of self-consistent Eq.(5) is obtained at $t=1$, we can quantify the contribution of node i to $\|v_{\rightarrow}\|$ for $t=1$, which is formulated by the content in brackets of Eq.(17). Let's define it as the Hypergraph Collective Influence (HCI) of node i to find the optimal influencers:

$$HCI_1(i) = k_i + \sum_{e_{\gamma} \in \partial i} \sum_{j \in \partial e_{\gamma}/i} I_{ie_{\gamma}e_{\gamma}j}^0 \quad (18)$$

As shown in Fig.(2b), we can calculate the $HCI_1(i)$ through Eq.(18), so $HCI_1(i) = 8$.

For $t=2$, based on Eq.(6), we have $\mathbf{V}_{\rightarrow}^2 = \mathbf{n}_{\rightarrow} + J\mathcal{G}^1 \times \mathbf{V}_{\rightarrow}^1 = \mathbf{n}_{\rightarrow} + J\mathcal{G}^1 \times \mathbf{n}_{\rightarrow} + J\mathcal{G}^1 \times J\mathcal{G}^0 \times \mathbf{n}_{\rightarrow}$, so:

$$\begin{bmatrix} \mathbf{v}_1 \\ \mathbf{v}_2 \end{bmatrix}^2 = \begin{bmatrix} \mathbf{n}_1 + \mathcal{M}^1 \mathcal{F}^0 \mathbf{n}_1 \\ \mathcal{F}^1 \mathbf{n}_1 \end{bmatrix} \quad (19)$$

Same as above, the specific form of Eq.(19) can be described as

$$\begin{cases} v_{i \rightarrow e_{\gamma}}^2 = n_i H_{ie_{\gamma}} + (1 - n_i) H_{ie_{\gamma}} \sum_{e_{\beta}} H_{ie_{\beta}} (1 - \delta_{e_{\gamma}e_{\beta}}) M_{e_{\beta}ie_{\gamma}}^1 \\ \quad \times \sum_k n_k H_{ke_{\beta}} (1 - \delta_{ki}) I_{ke_{\beta}e_{\beta}i}^0 \\ v_{e_{\gamma} \rightarrow i}^2 = H_{ie_{\gamma}} \sum_j n_j H_{je_{\gamma}} (1 - \delta_{ij}) I_{je_{\gamma}e_{\gamma}i}^1 \end{cases} \quad (20)$$

Let us compute the Hypergraph Collective Influence of node i for $t=2$, the same process as above, we have:

$$\begin{aligned}
 HCI_2(i) &= k_i + \sum_{e_{\gamma} \in \partial i} \sum_{j \in \partial e_{\gamma}/i} I_{ie_{\gamma}e_{\gamma}j}^1 \\
 &+ \sum_{e_{\gamma} \in \partial i} \sum_{j \in \partial e_{\gamma}/i} I_{ie_{\gamma}e_{\gamma}j}^0 \sum_{e_{\mu} \in \partial j/e_{\gamma}} (1 - n_j) M_{e_{\gamma}jje_{\mu}}^1 \quad (21)
 \end{aligned}$$

As shown in Fig.(2c), the additional 3-length paths also contribute to $HCI_2(i)$, making $HCI_2(i)=12$. Due to the periodicity of $I_{ie_{\gamma}e_{\gamma}j}^1$, we can replace the $I_{ie_{\gamma}e_{\gamma}j}^1$ with $I_{ie_{\gamma}e_{\gamma}j}^0$. Therefore, the right part of the first line in Eq.(21) is actually the $HCI_1(i)$. Moreover, k_i can also be seen as $HCI_0(i)$, which corresponds to the High Hyper Degree (HHD) ranking. It is obvious that HCI_{t+1} is composed of HCI_t and all message of subcritical path with length t . So we can generalize the above HCI formula to any given $t=n$. In summary, based on Eq.(6), we

have $\mathbf{V}_{\rightarrow}^n = \mathbf{n}_{\rightarrow} + J\mathcal{G}^{n-1} \times \mathbf{V}_{\rightarrow}^{n-1} = [1 + \sum_{i=1}^n \prod_{j=1}^i J\mathcal{G}^{n-j}] \times \mathbf{n}_{\rightarrow}$, and for $n > 2$:

$$\begin{bmatrix} \mathbf{v}_1 \\ \mathbf{v}_2 \end{bmatrix}^n = \begin{bmatrix} \mathbf{n}_1 + \left(\sum_{L \in A_n} \prod_{l \in A_L} \mathcal{M}^{n-l+1} \mathcal{F}^{n-l} \right) \mathbf{n}_1 \\ \mathcal{F}^{n-1} \left(\mathbf{n}_1 + \left(\sum_{L \in A_n} \prod_{l \in A_L} \mathcal{M}^{n-l} \mathcal{F}^{n-l-1} \right) \mathbf{n}_1 \right) \end{bmatrix} \quad (22)$$

where $A_n = \{x \in N^+ | x \bmod 2 = 0, x \leq n\}$. By analyzing the Eq.(22) we can get the Hypergraph Collective Influence of node i for $t=n$:

$$HCI_n(i) = k_i + \sum_{L \in A_n} \mathbb{O}_L^n + \sum_{L \in B_n} \mathbb{E}_L^n \quad (23)$$

where $B_n = \{x \in N^+ | x \bmod 2 = 1, x \leq n\}$, \mathbb{O}_L^n and \mathbb{E}_L^n are defined as follows:

$$\begin{aligned} \mathbb{O}_L^n = & \sum_{e_{\gamma_1} \in \partial i_1} \sum_{i_2 \in \partial e_{\gamma_1}/i_1} I_{i_1 e_{\gamma_1} e_{\gamma_1} i_2}^{n-L} \sum_{e_{\gamma_2} \in \partial i_2/e_{\gamma_1}} (1 - n_{i_2}) M_{e_{\gamma_1} i_2 i_2 e_{\gamma_2}}^{n-L+1} \\ & \times \cdots \times \sum_{i_\ell \in \partial e_{\gamma_{\ell-1}}/i_{\ell-1}} I_{i_{\ell-1} e_{\gamma_{\ell-1}} e_{\gamma_{\ell-1}} i_\ell}^{n-2} \sum_{e_{\gamma_\ell} \in \partial i_\ell/e_{\gamma_{\ell-1}}} (1 - n_{i_\ell}) M_{e_{\gamma_{\ell-1}} i_\ell i_\ell e_{\gamma_\ell}}^{n-1} \end{aligned} \quad (24)$$

$$\begin{aligned} \mathbb{E}_L^n = & \sum_{e_{\gamma_1} \in \partial i_1} \sum_{i_2 \in \partial e_{\gamma_1}/i_1} I_{i_1 e_{\gamma_1} e_{\gamma_1} i_2}^{n-L} \sum_{e_{\gamma_2} \in \partial i_2/e_{\gamma_1}} (1 - n_{i_2}) M_{e_{\gamma_1} i_2 i_2 e_{\gamma_2}}^{n-L+1} \\ & \times \cdots \times \sum_{i_{\ell+1} \in \partial e_{\gamma_\ell}/i_\ell} I_{i_\ell e_{\gamma_\ell} e_{\gamma_\ell} i_{\ell+1}}^{n-1} \end{aligned} \quad (25)$$

Here $\ell = \frac{L+2}{2}$ and $t = \frac{L+1}{2}$. \mathbb{O}_L^n and \mathbb{E}_L^n represent the number of subcritical path starting from node i with odd and even length respectively, and both length of them do not exceed $n + 1$. Inspired by above, we define the concept of subcritical paths. For a directed link $i_1 \rightarrow e_{\gamma_1} \rightarrow \dots \rightarrow e_{\gamma_\ell}$ is a subcritical path of length $2\ell - 1$, if $n_{i_1} = 1, n_{i_2} = 0, \dots, n_{i_\ell} = 0, I_{i_1 e_{\gamma_1} e_{\gamma_1} i_2} = 1, M_{e_{\gamma_1} i_2 i_2 e_{\gamma_2}} = 1, \dots, I_{i_{\ell-1} e_{\gamma_{\ell-1}} e_{\gamma_{\ell-1}} i_\ell} = 1, M_{e_{\gamma_{\ell-1}} i_\ell i_\ell e_{\gamma_\ell}} = 1$. Same as above, the directed link $i_1 \rightarrow e_{\gamma_1} \rightarrow \dots \rightarrow i_\ell$ is a subcritical path of length $2\ell - 2$, if $n_{i_1} = 1, n_{i_2} = 0, \dots, n_{i_\ell} = 0, I_{i_1 e_{\gamma_1} e_{\gamma_1} i_2} = 1, M_{e_{\gamma_1} i_2 i_2 e_{\gamma_2}} = 1, \dots, I_{i_{\ell-1} e_{\gamma_{\ell-1}} e_{\gamma_{\ell-1}} i_\ell} = 1$. For locally tree-like hypergraphs, HCI_n can be approximately defined as the number of subcritical paths starting from i with length $0 \leq l \leq n$.

C. HCI-TM Algorithm

Our objective is to identify the most effective configuration of seeds \mathbf{n} , with a given size of qN , in order to maximize $\|v_{\rightarrow}\|$. By increasing the number of iterations or the time parameter n , we can obtain increasingly accurate approximations of the final state defined by Eq.(5). This signifies improved performance of $HCI_n(i)$. However, it also leads to an increase in the complexity of $HCI_n(i)$, as it becomes dependent on time and other seeds. In order to select the optimal influence node, we have devised an adaptive HCI-TM algorithm that follows a greedy approach based on the aforementioned analysis:

It is important to note that a_r represents the expected proportion of active nodes. In order to save computational resources, it is not necessary to update the HCI for all nodes. Instead, we only need to recalculate the neighbors within the $\lceil n/2 \rceil$ -layer of nodes that were activated in the previous step. This approach allows us to focus on the relevant nodes and optimize the efficiency of the algorithm.

IV. NUMERICAL SIMULATION:

In this section, we have conducted a comprehensive evaluation of the HCI-TM algorithm by comparing it with several

Algorithm 1: HCI_n-TM algorithm

Input:

Hypergraph: $\mathbb{H}(V, E)$,
Activation Radio: a_r

Output:

Seed Set: S

Initialization: $S = \emptyset$, Calculate the HCI_n values of all nodes in the hypergraph;

while $Q(q) < a_r$ **do**

Select node i with the highest HCI_n as the seed;

$S = \{i\} \cup S$;

Remove the newly activated node and hyperedge from the hypergraph;

Recalculate the HCI_n value of $\lceil n/2 \rceil$ -layer neighbor of node removed in the previous step;

end

return S

classical algorithms, namely HHD (High Hyper Degree Algorithm), HHDA (High Hyper Degree Adaptive Algorithm), NP (Neighbor Preference Algorithm), NPA (Neighbor Preference Adaptive Algorithm), PageRank, and RA (Random Algorithm). To ensure the robustness of our findings, we performed simulations on both synthetic and real-world hypergraphs. Our results revealed that the HCI-TM algorithm outperformed the other algorithms in various aspects. Specifically, it achieved maximum activation of the hypergraph while selecting a minimal seed set, thereby demonstrating its superior performance in the threshold models. It is worth noting that the parameter a_r was set to 0.9 in all experiments. This choice takes into account the presence of challenging-to-activate peripheral nodes in the hypergraphs.

A. Synthetic hypergraphs

To evaluate the effectiveness and efficiency of the HCI-TM algorithm, a series of experiments were conducted on synthetic hypergraphs. These hypergraphs consisted of Erds-Rényi (ER) hypergraphs³³ with average hyperdegrees of 2 and 3, Scale-Free (SF) hypergraphs²¹ with power-law exponent of 1.5 and 2, as well as K-uniform hypergraphs with hyperedge sizes of 4 and 5. The experiments covered a range of hypergraph size, including 5000, 10000, 20000, 30000, 50000, and 100000. The result of the experiment was averaged ten times to ensure the reliability of the results. All numerical simulations was conducted in giant connected component of hypergraphs based on our threshold rules.

FIG (3) illustrates the performance of various algorithms in ER, SF, and K-UF hypergraphs under different parameter settings, with a threshold of $t_\gamma = 0.5$. As depicted in FIG (3), the HCI-TM algorithm outperforms other algorithms in all cases. It achieves a node activation rate of 90% in the hypergraphs with the minimum number of seeds. The HHDA algorithm performs relatively good performance, ranking second in terms of effectiveness, while the RA algorithm need select the most seed nodes. Through our experimental simulations, we observed that the superiority of HCI-TM algo-

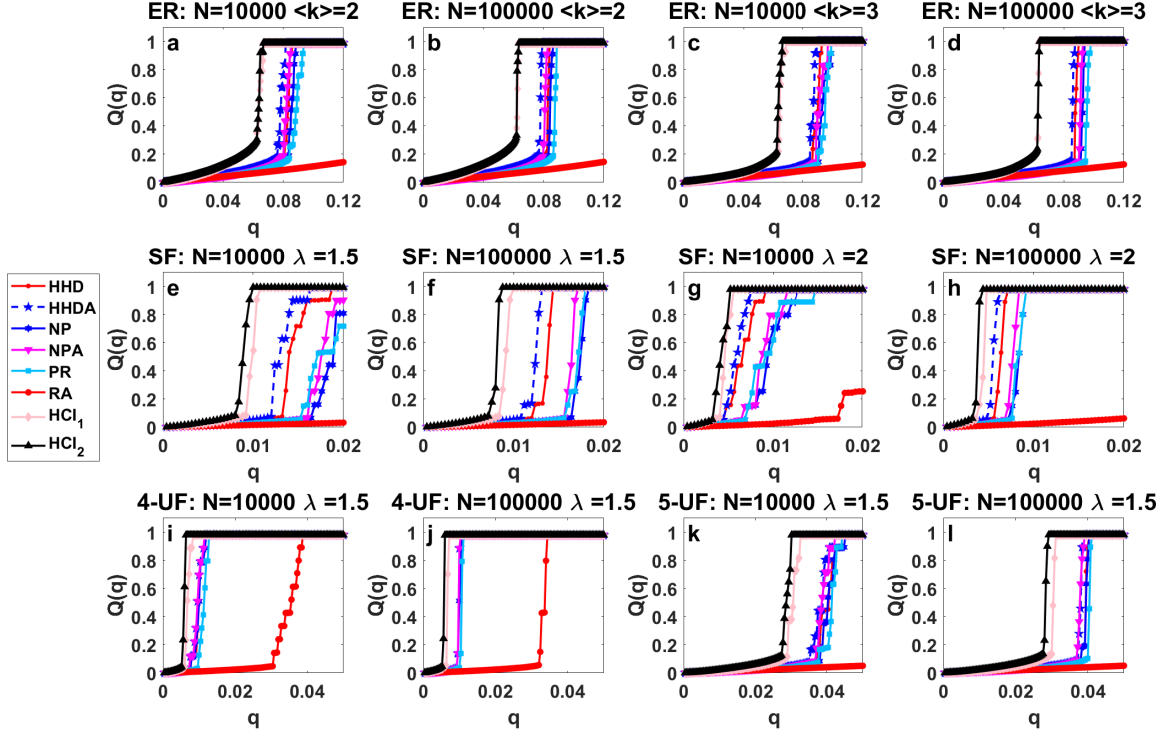


FIG. 3. Performance of HCI-TM algorithm and other algorithms on ER, SF and K-UF hypergraphs. The size of hypergraphs N are 10000 and 100000, and $M = 0.3N$ in ER hypergraphs, $M = 0.5N$ in SF and K-uniform hypergraphs. The horizontal axis of each subfigure represents the proportion of seed nodes in the hypergraphs, and the vertical axis represents the proportion of active nodes in the hypergraphs.

rithm becomes increasingly evident in ER hypergraphs as the average hyperdegree increases. However, the performance of the HCI-TM algorithm on SF hypergraphs deteriorates as the power-law exponent increases. This phenomenon can be attributed to that the larger power-law exponent limits the number of nodes with large hyperdegrees, causing the more hyperdegree of nodes to be 1, making the failure of the HCI-TM algorithm.

FIG (4) presents the proportion of seed nodes required by different algorithms to achieves 90% node activation in ER, SF, and K-uniform hypergraphs. As shown in FIG (4), the HCI-TM algorithm consistently outperforms other algorithms by selecting optimal influence seed sets with the minimum number of nodes. Following the HCI-TM algorithm, the HHDA algorithm demonstrates relatively good performance, while the RA algorithm requires the largest number of seed nodes. These results highlight the effectiveness of the HCI-TM algorithm in identifying influential nodes in the hypergraphs, allowing it to achieve a high activation rate while minimizing resource utilization.

In order to evaluate the effectiveness of HCI, we conducted an analysis of HCI_n during the spreading process. Initially, we examined the evolution of HCI based on the HCI-TM ranking during sequential activation, as shown in FIG (5). It can be observed that in the early stages, the HCI value is small and there is a little disparity between HCI_1 and HCI_2 . However,

TABLE I. The TABLE show the slope of different algorithm running times using a one order polynomial fitting on different types of hypergraphs.

Algorithms	HHD	HHDA	NP	NPA	PR	RA	HCI_1	HCI_2
ER-2	1.28	1.03	1.17	0.76	0.87	1.04	1.02	1.03
ER-3	1.25	1.03	1.13	0.83	0.92	1.02	1.02	1.03
SF-1.5	1.07	1.02	1.06	0.73	0.95	1.04	1.07	1.07
SF-2	1.04	1.01	1.03	0.64	0.89	1.02	1.03	1.06
4-UF	1.06	1.01	1.04	0.58	0.92	1.00	1.02	1.01
5-UF	1.16	1.02	1.10	0.70	0.97	1.04	1.03	1.04

as the propagation process unfolds, the gap between HCI_1 and HCI_2 gradually widens. Furthermore, our findings indicate that the occurrence of the cascade phenomenon corresponds to the peak evolution of HCI. Notably, the peak of HCI_2 occurs earlier and reaches a higher value compared to HCI_1 . Remarkably, the HCI_2 algorithm achieves this superior performance while utilizing fewer seed nodes. These results demonstrate the significant impact of HCI in the cascading process and suggest that it can be used as a tool to predict the occurrence of cascading phenomenon.

We recorded the computational time of each algorithm in different synthetic hypergraphs. The logarithm (\log_{10}) of the computational time and the scale of the hypergraph were then calculated. Subsequently, we plotted a line graph with the

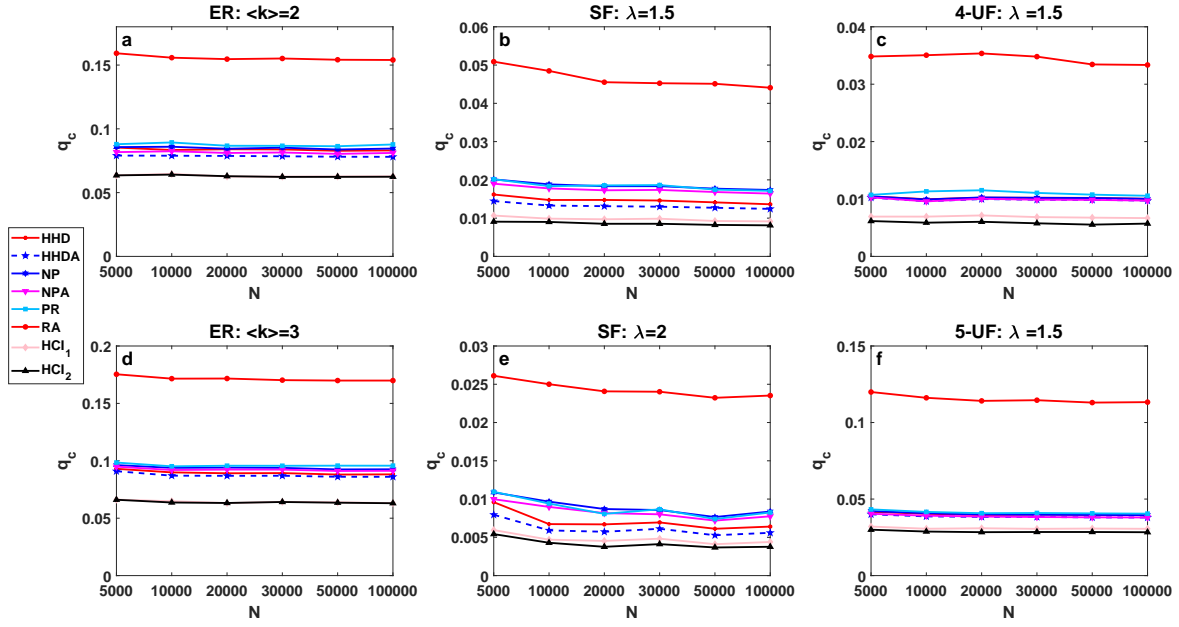


FIG. 4. The fraction of seed nodes required by different algorithms to activate the ER hypergraphs with the average hyperdegree of 2 and 3, the SF hypergraphs with the power-law exponent of 1.5 and 2 and the K-uniform hypergraphs with the size of hyperedges are 4 and 5. The horizontal axis represents the hypergraph size, and the vertical axis represents the proportion of seed nodes.

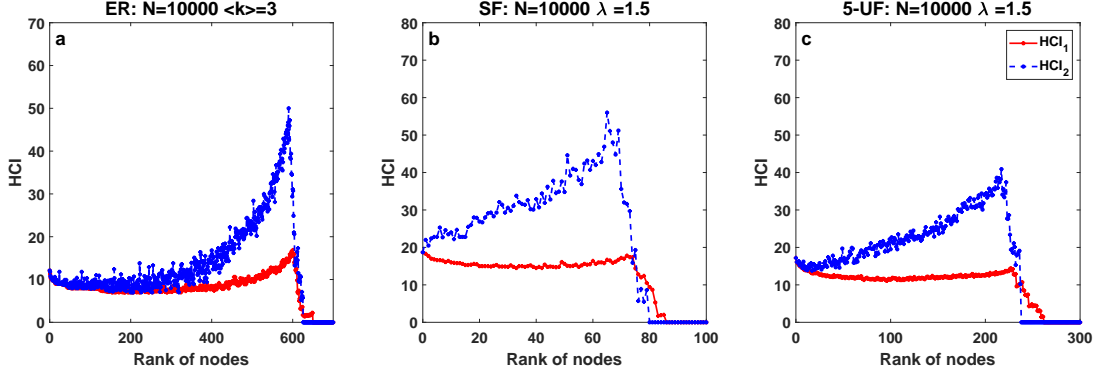


FIG. 5. Analysis of the HCl value attached to each node when it is activated sequentially according to HCl_n -TM ranking. a-c shows the results of HCl algorithm on ER hypergraphs with average hyperdegree of 3, SF hypergraphs with the power-law exponent of 1.5 and UF hypergraphs with size of hyperedges are 5, and the size of hypergraphs N are 10000.

scale of hypergraph on the horizontal axis and the time on the vertical axis, as shown in FIG (6). To analyze the time complexity of the algorithms, we fitted the running time data with first-order polynomials, as presented in TABLE (I). Our analysis revealed that the time consumed by each algorithm exhibits a linear growth pattern in relation to the hypergraph size. Remarkably, the HHD algorithm exhibits the highest time complexity, approximately $O(N^{1.14})$, while the NPA algorithm demonstrates the lowest time complexity, approximately $O(N^{0.71})$. The time complexity of the HCl-TM algorithm, approximately $O(N^{1.04})$, demonstrates a linear increase in computational time as the scale of the hypergraph increases. Among all the algorithms examined, the PageRank algorithm

consumes the most time, while the RA algorithm exhibits the lowest time complexity. The HCl-TM algorithm strikes a reasonable balance between time complexity and performance, making it a pragmatic choice for practical applications.

B. Real-world hypergraphs

The threshold models in hypergraphs is widely utilized in various real-world scenarios, encompassing the proliferation of public opinion and protein interaction hypergraphs. In this subsection, we conducted six numerical simulations in real-world hypergraphs to demonstrate the efficacy of the HCl-TM

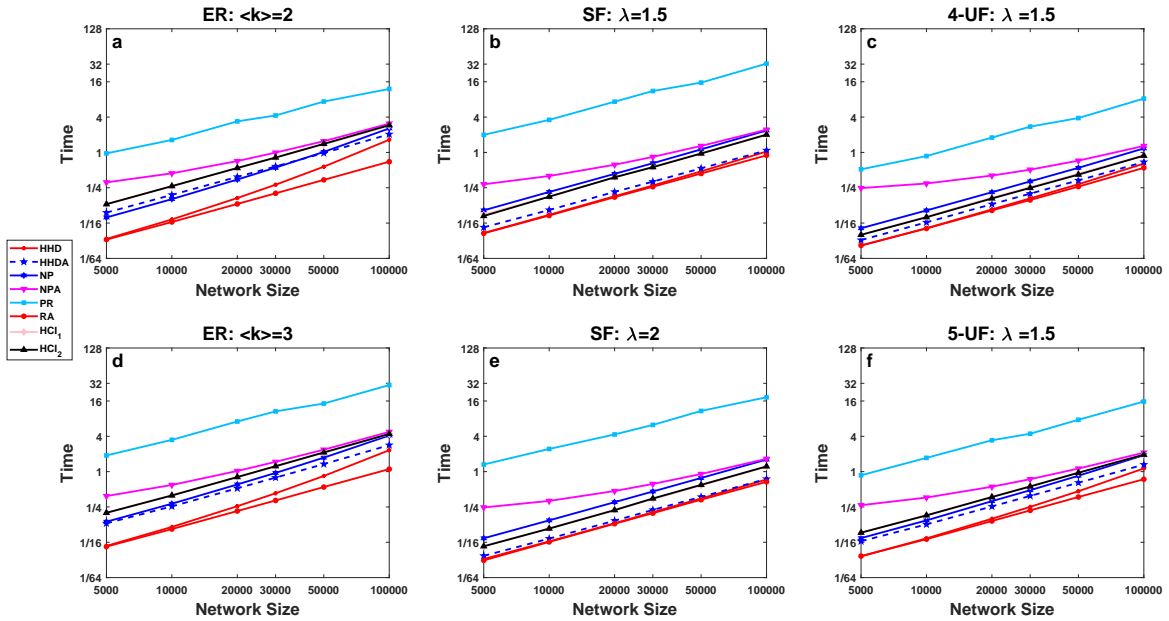


FIG. 6. The computational time (seconds) of different algorithms on ER hypergraphs, SF hypergraphs and the K-uniform hypergraphs. The horizontal axis is $\log_{10}(N)$, and the vertical axis is $\log_{10}(T)$, where N represent the number of node in the hypergraphs and T represent computational time.

algorithm. The specific information about the real-world hypergraphs is presented in TABLE (II).

TABLE II. Some specific information about the real-world hypergraphs dataset, including the number of nodes and hyperedges, and the threshold settings.

Dataset	N	M	t_γ
House-committees	1,290	341	0.6
Vegas-bars-reviews	1,234	1,194	0.6
Geometry-questions	580	1,193	0.8
Senate-committees	282	315	0.8
MAG-10	80,198	51,889	0.5
Mathoverflow-answers	73,851	5,446	0.5

The first dataset we used is Congressional data compiled by Charles Stewart and Jonathan Vaughan³⁴. The nodes of the House-Committees dataset represent members of the U.S. house of Representatives, and the hyperedges represent the committee members. There are 1290 nodes and 341 hyperedges in the hypergraph, and the average and median number of nodes in each hyperedges are 34.8 and 40 respectively.

As depicted in FIG (7a), we can observe the performance of the HCI-TM algorithm in comparison to other classical algorithms. Specifically, when applied to the US Congressional hypergraph, the HCI-TM algorithm excels by achieving full activation at an early stage. Notably, HCI₁ and HCI₂ outperform all other algorithms by selecting 75 seed nodes. Among the alternative algorithms, the HHDA algorithm demonstrates the third-best performance, achieving full activation with 102 seed nodes. However, there is still a significant gap compared

to the HCI-TM algorithm. On the other hand, the RA algorithm need to select 34.4% seed nodes (approximately 444 nodes). This striking example effectively highlights the substantial advantages of the HCI-TM algorithm, underscoring its practical utility and application value.

The Vegas-bars-reviews dataset³⁵ is derived from the Yelp Kaggle competition data which node represents the user, and hyperedge contains lists of reviewers that reviewed a certain type of establishment within a month. In FIG (7b), the superiority of the HCI-TM algorithm over other classical algorithms on the Vegas-bars-reviews dataset is clearly demonstrated. As the hypergraph reaches 90% activation, the HCI₁-TM algorithm and HCI₂-TM algorithm select 82 and 49 seed nodes respectively, while the HHDA algorithm and NPA algorithm select 124 and 136 seed nodes respectively. Comparing with the HHDA algorithm and NPA algorithm, the HCI algorithm exhibits remarkable advantages, which become more pronounced as the order of the HCI algorithm increases. Among all the algorithms compared, the NP algorithm performs the poorest, requiring 567 seed nodes.

The third real-world hypergraph is the Geometry-question dataset³⁵. The nodes represent the users of MathOverflow and hyperedges are sets of users who answered a certain question category. FIG (7c) presents the performance of various algorithms on the Geometry-question dataset. The results clearly indicate that the HCI-TM algorithm outperforms all other algorithms. Notably, the HCI₂-TM algorithm achieves a hypergraph activation rate of over 90% by selecting only 20 nodes, which is nearly 45% higher than the performance of the HHDA algorithm.

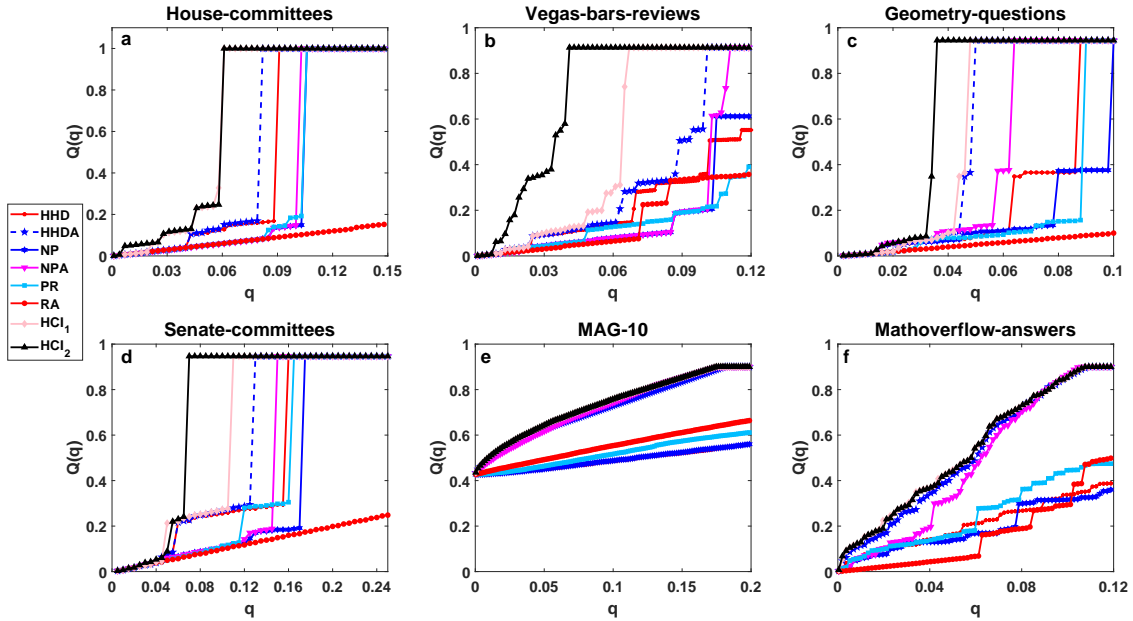


FIG. 7. Performance of HCI-TM algorithm and other classical algorithms on real-world hypergraphs. And the horizontal axis represent the proportion of seed nodes and the vertical axis represent the proportion of active nodes in the hypergraph.

The fourth dataset is Senate-Committees³⁴, which nodes represent the members of the United States senate and the hyperedges correspond to committee members. The performance of different algorithms are showed in Fig.(7d), and it outperforms all others. Compared to other classical algorithms, the HCI₂-TM algorithm only select 19 seed nodes to achieve the same goal, whereas the HHDA algorithm, which exhibits the best performance among the other classical algorithms, required 36 seeds. That clearly demonstrates the superiority of the HCI-TM algorithm.

The MAG-10 dataset^{36,37} comprises authors as nodes and their corresponding publications as hyperedges within the Microsoft Academic Graph subset. Fig(7e) shows that all algorithms could activate the hypergraph to 0.4 using very few seeds at the initial stage. As propagation process evolved, we observed that the HCI-TM algorithm exhibits a slight advantage over other algorithms. However, HCI-TM algorithm is surpassed by the NPA and HHDA algorithms in the final stage, but the gap between them was very small. The last dataset we selected was Mathoverflow-answers³⁸, where the nodes represent the user, and the hyperedges are the set of questions answered by the users. As can be seen from Fig.(7f), HCI-TM algorithm has obvious advantages compared with other algorithms in the initial stage. However, as the propagation process evolved, the difference between the HCI-TM algorithm and the HHDA and NPA algorithms gradually diminished. In the final stage, NPA algorithm is slightly ahead of HCI-TM algorithm. In addition, we found no first-order phase transitions in the MAG-10 and Mathoverflow-answers datasets when the threshold was set to 0.5. All experiments in real-world hypergraphs show that HCI-TM has strong robustness and superi-

ority.

V. CONCLUSION:

The Influence Maximization problem in hypergraphs has gained attention due to its relevance in real-world scenarios involving high-order interactions. However, this field is still in its early stages, with many heuristic approaches lacking sufficient mathematical analysis and neglecting the dependence of nodes' neighbors. This paper focuses on optimizing node influence based on the threshold models in hypergraphs, but it only solves specific problems. Future research will investigate more general probabilistic agent-based HCI-TM algorithms, applying a message passing theoretical analysis framework to address a broader range of spread and diffusion problems in hypergraphs.

Additionally, the structure of the hypergraphs may have an impact on the occurrence of the cascade phenomenon, which is an area of focus for our future research. Understanding how different hypergraph structures influence the dynamics of information spreading and the cascade phenomenon can provide valuable insights into optimizing Influence Maximization strategies. By further investigating this aspect, we aim to uncover additional factors that contribute to the spread of influence in hypergraphs and develop more effective algorithms for Influence Maximization problem.

ACKNOWLEDGMENTS

We wish to acknowledge the support from the National Key Research and Development Program of China (Grant No.2021ZD0112400), National Natural Science Foundation of China (Grant No.12371516), Liaoning Provincial Natural Science Foundation (Grant No.2022-MS-152), Fundamental Research Funds for the Central Universities(DUT22LAB305).

Appendix A: Compared Algorithm

To assess the efficacy of the HCI-TM algorithm, we employed several established algorithms that are commonly utilized in pairwise networks and extended them for application in hypergraphs. Through a comparative analysis with other classical algorithm, we substantiate the superior performance of HCI-TM in efficiently selecting the most influential nodes, thus achieving maximum propagation scale within the hypergraphs.

Neighbor Preference Algorithm(NP):

The NP algorithm employs a sorting technique to prioritize nodes based on their one-layer neighbor count, selecting the node with the highest number of neighbors as the initial seed node for spreading. This process continues until a specific proportion of nodes in the hypergraphs are activated. In order to enhance its efficiency, the NPA algorithm builds upon this approach. After each removal, the neighbors of each node are recalculated, and unactivated nodes with the highest number of neighbors are chosen as seed. Notably, the NPA algorithm avoids selecting already activated nodes as seeds, further optimizing the NP algorithm. The algorithm terminates once the desired proportion of nodes in the hypergraphs are activated.

High Hyper Degree Algorithm(HHD):

The HHD algorithm ranks nodes in descending order based on their hyperdegree and selects the node with the highest hyperdegree as the initial seed node for propagation in the hypergraph. This process continues until a specified proportion of nodes in the hypergraphs are activated. HHDA algorithm is an improvement of HHD algorithm. After each removal, the hyperdegree of each node is recalculated, and the HHDA algorithm prioritizes selecting the remaining unactivated node with the highest hyperdegree as the seed. The algorithm terminates when the desired proportion of nodes in the hypergraphs are activated. By reducing the overlap of already activated nodes as seeds during propagation, the HHDA algorithm enhances the efficiency of the HHD algorithm.

PageRank(PR):

The PageRank algorithm is a widely used method employed by the Google search engine to evaluate the significance of web pages. It operates by analyzing the linkage relationships between web pages, providing a measure of their relative importance in search engine rankings. In our study, we have extended the conventional PageRank algorithm from pairwise networks to hypergraphs, and the PageRank value of each node in the hypergraph can be defined as follows:

$$\begin{cases} PR(i) = d \left(\sum_{j \in \ell i} \frac{PR(j)}{L(j)} \right) + \frac{1-d}{N} \\ L(j) = \sum_{e_\gamma \in \partial j} N_\gamma - 1 \end{cases} \quad (A1)$$

In Eq.(A1), ℓi represents the first layer neighbors of a node, N_γ represents the number of nodes in the hyperedge e_γ , and $d \in (0, 1)$ is the damping factor. The PageRank value of each node in the hypergraph is iteratively updated based on the aforementioned equation until convergence is achieved. Once convergence is reached, the nodes are sorted based on their PageRank values. The node with the highest PageRank value is selected as the seed node to activate the hypergraph. The algorithm terminates until a specific proportion of nodes in the hypergraph are activated.

Random Algorithm(RA):

The random algorithm selects seed nodes randomly and propagates them in the hypergraphs. The algorithm terminates until a specific proportion of nodes in the hypergraphs are activated.

REFERENCES

- ¹Granovetter and Mark, "Threshold models of collective behavior," *American Journal of Sociology* **83**, 1420–1443 (1978).
- ²E. Tardos, D. Kempe, and J. Kleinberg, "Maximizing the spread of influence in a social network," 9th ACM SIGKDD International Conference on Knowledge Discovery and Data Mining **1**, 1–10 (2003).
- ³T. W. Valente and R. L. Davis, "Accelerating the diffusion of innovations using opinion leaders," *Annals of the American Academy of Political & Social Science* **566**, 55–67 (1999).
- ⁴A. Galeotti and S. Goyal, "Influencing the influencers: a theory of strategic diffusion," *Rand Journal of Economics* **40**, 509–532 (2010).
- ⁵C. Chen, Wei Wang and Y. Wang, "Scalable influence maximization for prevalent viral marketing in large-scale social networks," in *Proceedings of the 16th ACM SIGKDD International Conference on Knowledge Discovery and Data Mining, Washington, DC, USA, July 25-28, 2010* (2010) pp. 1–11.
- ⁶"Targeted influence maximization in complex networks," *Physica D: Nonlinear Phenomena* **446**, 133677 (2023).
- ⁷H. Huang and H. He, "Community-based influence maximization for viral marketing," *Applied Intelligence: The International Journal of Artificial Intelligence, Neural Networks, and Complex Problem-Solving Technologies* **49**, 2137–2150 (2019).
- ⁸S. Lei, "Online influence maximization," *ACM* , 645.654 (2015).
- ⁹F. Morone, H. A. Makse, J. Wang, and S. Pei, "Influencer identification in dynamical complex systems," (2020).

- ¹⁰S. Pei, L. Muchnik, J. S. Andrade, Z. Zheng, and H. A. Makse, “Searching for superspreaders of information in real-world social media,” *Scientific reports* **4**, 5547 (2014).
- ¹¹Linton, C., and Freeman, “Centrality in social networks conceptual clarification,” *Social Networks* **1**, 215–239 (1978).
- ¹²H. Albert, R. Jeong and A. Barabási, “Error and attack tolerance of complex networks,” *Elsevier B.V.* **406**, 378–382 (2000).
- ¹³S. Brin and L. Page, “The anatomy of a large-scale hypertextual web search engine,” *Computer Networks and ISDN Systems* **30**, 107–117 (1998).
- ¹⁴S. B. Seidman, “Network structure and minimum degree,” *Social Networks* **5**, 269 (1983).
- ¹⁵F. Morone and H. Makse, “Influence maximization in complex networks through optimal percolation,” *Nature* **527**, 65 (2015).
- ¹⁶S. Pei, X. Teng, J. Shaman, F. Morone, and H. A. Makse, “Efficient collective influence maximization in cascading processes with first-order transitions,” (2016).
- ¹⁷R. Zhang and S. Pei, “Dynamic range maximization in excitable networks,” *Chaos: An Interdisciplinary Journal of Nonlinear Science* **28**, 013103 (2018).
- ¹⁸R. J. Martinez, N. D. Williams and J. A. Dunne, *SANTA FE INSTITUTE STUDIES IN THE SCIENCES OF COMPLEXITY - PROCEEDINGS VOLUMES* (2006).
- ¹⁹F. Battiston, G. Cencetti, I. Iacopini, V. Latora, M. Lucas, A. Patania, J. G. Young, and G. Petri, “Networks beyond pairwise interactions: Structure and dynamics,” (2020).
- ²⁰D. Zhou, J. Huang, B. S. Olkoph, and B. Schkopf, “Beyond pairwise classification and clustering using hypergraphs,” in *Computer Vision and Pattern Recognition, 2005. CVPR 2005. IEEE Computer Society Conference on* (2005) pp. 1–14.
- ²¹M. X. X.-X. Z. C. Liu and Z.-K. Zhang., “An efficient adaptive degree-based heuristic algorithm for influence maximization in hypergraphs,” *Information Processing & Management* **60**, 103161 (2023).
- ²²A. Antelmi, G. Cordasco, C. Spagnuolo, and P. Szufel, “Social influence maximization in hypergraphs,” *Entropy* **23**, 796 (2021).
- ²³A. R. Benson, “Three hypergraph eigenvector centralities,” *SIAM Journal on Mathematics of Data Science* **1**, 293–312 (2019).
- ²⁴M. E. Aktas, S. Jawaid, I. Gokalp, and E. Akbas, “Influence maximization on hypergraphs via similarity-based diffusion,” in *2022 IEEE International Conference on Data Mining Workshops (ICDMW)*, Vol. 22 (2022) pp. 1197–1206.
- ²⁵F. Tudisco and D. Higham, “Node and edge nonlinear eigenvector centrality for hypergraphs,” **4**, 1–10 (2021).
- ²⁶B. Karrer and M. E. J. Newman, “Message passing approach for general epidemic models,” *Phys. Rev. E* **82**, 016101 (2010).
- ²⁷Y.-H. Cheng, Chun-Hung. Kuo and Z. Zhou, “Outbreak minimization v.s. influence maximization: an optimization framework,” *BMC Medical Informatics and Decision Making* **20** (2020).
- ²⁸Z. Wei and M. S. He, “Influence of opinion leaders on dynamics and diffusion of network public opinion,” in *International Conference on Management Science and Engineering-Annual Conference Proceedings* (2013).
- ²⁹L. Vassio, F. Fagnani, P. Frasca, and A. Ozdaglar, “Message passing optimization of harmonic influence centrality,” *IEEE Transactions on Control of Network Systems* **1**, 109–120 (2014).
- ³⁰D. Centola, “The spread of behavior in an online social network experiment,” *Science* **329**, 1194–1197 (2010).
- ³¹S. Aral and D. Walker, “Creating social contagion through viral product design: A randomized trial of peer influence in networks,” *Management Science* **57**, 44 (2011).
- ³²L.-J. Z. Xin-Jian Xu, Shuang He, “Dynamics of the threshold model on hypergraphs,” *Chaos* **32**, 023125 (2022).
- ³³S. Aksoy, T. G. Kolda, and A. Pinar, “Measuring and modeling bipartite graphs with community structure,” *Journal of Complex Networks* (2016).
- ³⁴P. S. C. N. Veldt and A. R. Benson, “Generative hypergraph clustering: From blockmodels to modularity,” *Science Advances* **7**, 1303 (2021).
- ³⁵I. Amburg, N. Veldt, and A. R. Benson, “Hypergraph clustering for finding diverse and experienced groups,” arXiv.2006.05645 (2020).
- ³⁶I. Amburg, N. Veldt, and A. Benson, “Clustering in graphs and hypergraphs with categorical edge labels,” in *WWW '20: The Web Conference 2020* (2020) pp. 706–17.
- ³⁷A. Sinha, Z. Shen, Y. Song, H. Ma, and K. Wang, “An overview of microsoft academic service (mas) and applications,” in *the 24th International Conference* (2015) pp. 243–246.
- ³⁸A. R. Veldt, N. Benson and J. Kleinberg, “Minimizing localized ratio cut objectives in hypergraphs,” *26th ACM SIGKDD International Conference on Knowledge Discovery and Data Mining (KDD)*, 1708–1718 (2020).
- ³⁹D. Watts, “A simple model of global cascades on random networks,” (2011) pp. 5766–5771.
- ⁴⁰J. M. Mcgloin and Z. R. Rowan, “A threshold model of collective crime,” *Criminology* **53**, 484–512 (2015).
- ⁴¹S. Hasan and S. V. Ukkusuri, “A threshold model of social contagion process for evacuation decision making,” *Transportation Research Part B Methodological* **45**, 1590–1605 (2011).
- ⁴²A. Xi, W. B. Peng, A. Xjx, and C. Gx, “Universal behavior of the linear threshold model on weighted networks,” *Journal of Parallel and Distributed Computing* **123**, 223–229 (2019).